INSTITUTE OF PHYSICS
FACULTY OF PHYSICS, ASTRONOMY
AND APPLIED COMPUTER SCIENCE
JAGIELLONIAN UNIVERSITY

Bachelor Thesis

Methods of searching for the dark matter boson

Krzysztof Kacprzak

Supervisor: Professor Paweł Moskal

Frascati 2011 – Cracow 2012

Contents

1 Introduction 2

2 Astrophysical observations 3

3 Dark Matter Theory 7
- 3.1 Lagrangian . . . 7
- 3.2 Sommerfelds enhancement . . . 7
- 3.3 More about secluded sector . . . 8

4 Methods of the search 10
- 4.1 Direct search . . . 10
- 4.2 Decays of mesons . . . 11
- 4.3 Fixed target experiments . . . 12
- 4.4 Search in the continuum processes . . . 13

5 Cross-section evaluation 15
- 5.1 Introduction . . . 16
- 5.2 $e^+e^- \to \mu^+\mu^-$ in QED . . . 19
- 5.3 $e^+e^- \to e^+e^-$ Bhabha events . . . 21
- 5.4 U boson exchange . . . 22
- 5.5 Inclusion of the background . . . 25
- 5.6 Feasibility study of the U boson observation . . . 26

6 Summary 28

7 Acknowledgements 28

8 Appendix 29
- 8.1 Definitions . . . 29
- 8.2 Calculations . . . 30

References 34

Abstract

The description of various methods of search for recently postulated dark matter boson, called U, is contained with explanation of origin and motivation for the ongoing, earth-bound search, followed by application of theoretical model of calculating cross-section for reaction $e^+e^- \to U(\gamma) \to \mu^+\mu^-(\gamma)$, based on Feynman diagram method. Integrated luminosity of e^+e^- collisions needed to observe the U boson were estimated as a function of two parameters: U boson mass m_U, kinetic-mixing parameter ϵ ($\epsilon^2 = \alpha'/\alpha$).

1 Introduction

Motivation for search of U boson is derived from several astrophysical observations, which separately can be explained, but on common ground they demand a new interpretation. Hypothesis of dark matter existence connected with these observations implies existence of "hidden sector" symmetry group $U(1)_d$. Dark matter cannot be observed directly, because it doesn't interact through electromagnetic forces, but there is proposed indirect way, through gauge vector U boson, which is supposed to couple two symmetry groups: $U(1)_Y$ of Standard Model (SM) and mentioned $U(1)_d$. According to this theory, there are states which are charged under both this groups: such particle has hypercharge Y and unknown dark matter charge d. Thus through kinetic mixing mediation between SM and hidden sector can be accomplished.

This thesis presents in general the current attempts of searching for the U boson. Chapter 2 and 3 consist of overview of astrophysical observations and discussion of theoretical basics of dark matter existence. In the following sections non-astrophysical methods of the search (based on particle physics experiments) are described, then the evaluation of cross-section for $e^+e^- \to U(\gamma) \to \mu^+\mu^-(\gamma)$ process is explained, which is preceded by introduction of Feynman diagram calculation method. The work is completed with summary and discussion of perspective for the experimental search for the U boson. Appendix contains necessary definitions and detailed calculations.

2 Astrophysical observations

Since postulation of dark matter existence in 1933 [1], there has been ongoing search for decisive proof. Such evidence was provided by Chandra telescope observation of a galactic cluster 1E0657-558 (Figure 1) [2]. Roentgen photograph acquired in 2002 by Markevitch *et al.* [3], in which there are vividly visible two emission centres, one of them in a shape of a bullet. It means, that in fact two galactic clusters are colliding with each other with great velocity. Distributions visible in Figure 1 indicate, that the regions of roentgen rays emission are not in the same place as gravitational centres. This fact is interpreted as galactic gas being decelerated and warmed up during collision (thus emitting roentgen radiation), while visible and dark matter just passing through. Additional measurements of gravitational potential distribution proves, that there has to be something interacting gravitationally more, than only light matter. The theory of modified gravity, which is not taking into account existence of dark matter, was not capable of explaining this observation, sole and thorough explanation is provided by Dark Matter Theory.

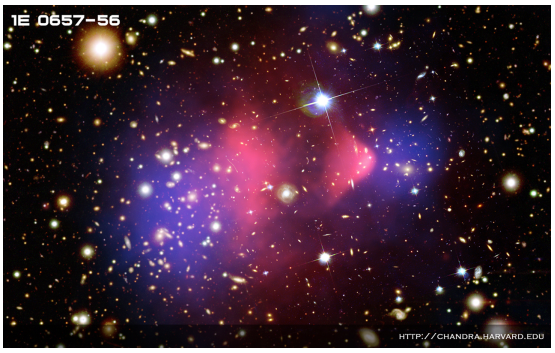

Figure 1: Two galactic clusters, numbered 1E0657-588. Roentgen radiation regions is coloured pink, reconstruction of dark matter distribution is blue. The gas cloud on the right is shaped like a bullet, proving, that a collision of two clusters underwent in the past. Figure adapted from chandra.harvard.edu.

This discovery does not complete the list of evidences, indicating a need for expanding Standard Model by new particles and interactions. Recent experiments have proven, that there exists source of positron and electron excess in the centre of our galaxy, that cannot be explained by supernova shocks. There are also other observations, indicating existence of dark matter, here are some examples:

1. PAMELA (Payload for Antimatter Matter Exploration and Light-nuclei Astrophysics) is designed to detect cosmic rays. It reported abundance of positrons in the range of 10-100 GeV [4] (Figure 2), in contrary to what is expected from high-energy cosmic rays interacting with the interstellar medium. This $N_{e^+}/(N_{e^+}+N_{e^-})$

excess is thought to be a sign of dark matter annihilation: hypothetical WIMPs (Weekly Interacting Massive Particles) colliding with and annihilating each other to e^+e^-.

2. ATIC (Advanced Thin Ionisation Calorimeter) is a balloon-borne cosmic ray detector, which studies electrons and positrons up to TeV energies. It reported a 4-6σ excess in its e^- data at energies of 300 - 800 GeV [5], as shown in Figure 2. Dark matter would seem a natural candidate explaining this observation well.

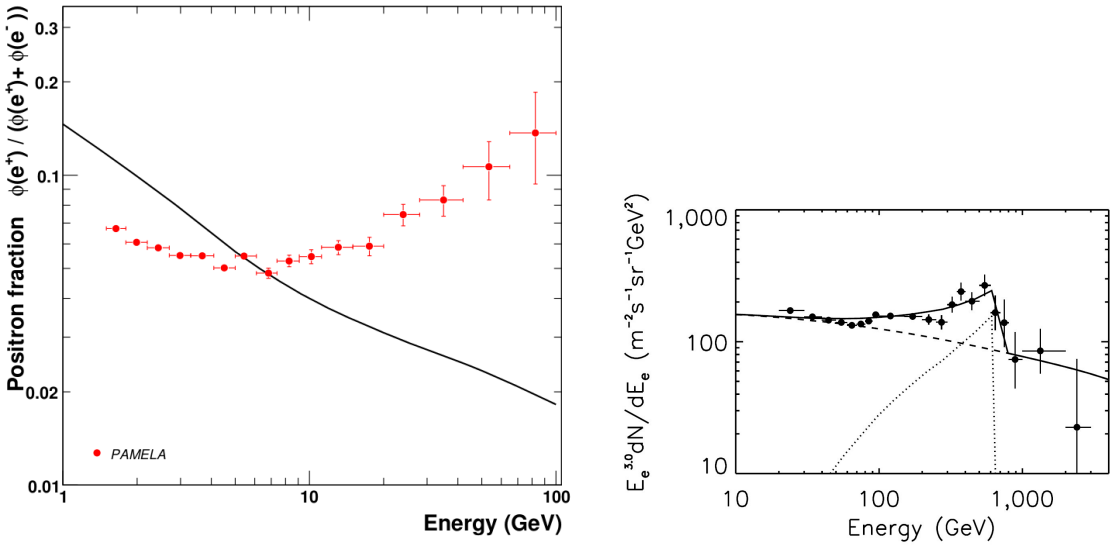

Figure 2: PAMELA and ATIC results. Left: PAMELA positron fraction compared with theoretical model. The solid line shows a calculation by Moskalenko and Strong for pure secondary production of positrons during the propagation of cosmic-rays in the galaxy. One standard deviation error bars are shown. Figure adapted from [4]. Right: ATIC high-energy electron counts. The triangular solid curve fitted to the data comes from a model of dark-matter annihilation featuring a Kaluza-Klein particle of mass near 620 GeV; dashed line shows model without a Kaluza-Klein particle and dotted triangular curve is difference between solid and dashed line. Figure derived from [5].

3. WMAP (Wilkinson Microwave Anisotropy Probe) [6] study of microwave emission from galactic centre show a component not spatially correlated with any known galactic emission mechanism. This "WMAP haze" can be explained as synchrotron radiation from electrons and positrons produced from dark matter annihilation in the galactic centre [7].

4. INTEGRAL (INTErnational Gamma-Ray Astrophysics Laboratory) has reported a 511 keV signal near the galactic centre, indicating new source of approximately $3 \times 10^{42} e^+$ annihilating per second, far more than expected from supernovae. This could be explained by annihilation of light $\mathcal{O}$(1-10 MeV) dark matter or by $\mathcal{O}$(100 GeV - 1 TeV) dark matter with $\mathcal{O}$(1 MeV) excited states.

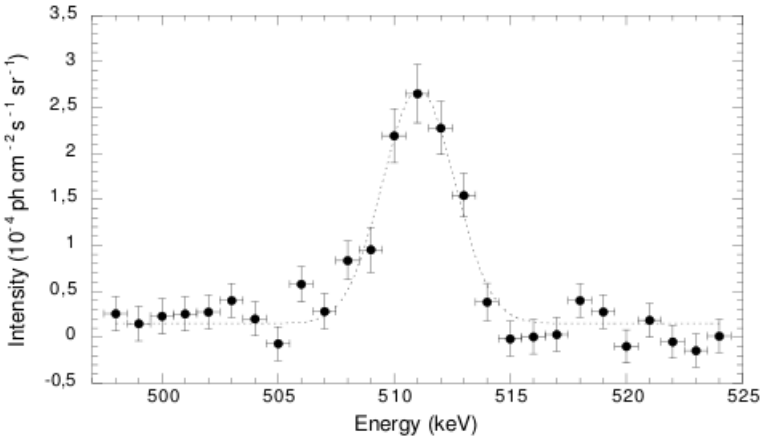

Figure 3: 511 keV flux spectrum observed by SPI/INTEGRAL. The photon spectrum (dotted line) was obtained by fitting Gaussian function with half-width of 10°. Figure adapted from [8].

5. DAMA/LIBRA is an experiment designed to detect recoil nuclei, which, among other processes, may originate from the scattering of Dark Matter particles with the nuclei in the detector material. The revolution of the Earth around the Sun can cause an annual modulation of the dark matter flux. This should give rise to an annual modulation in the number of detected recoils over a constant background. Thus provides a simple way to extract a dark matter signal from the background. Reported annual modulation of the signal (see Figure 4) could be explained by hypothesis, that dark matter-nucleus scattering is dominated by an inelastic process: $\chi N \to \chi^* N$.

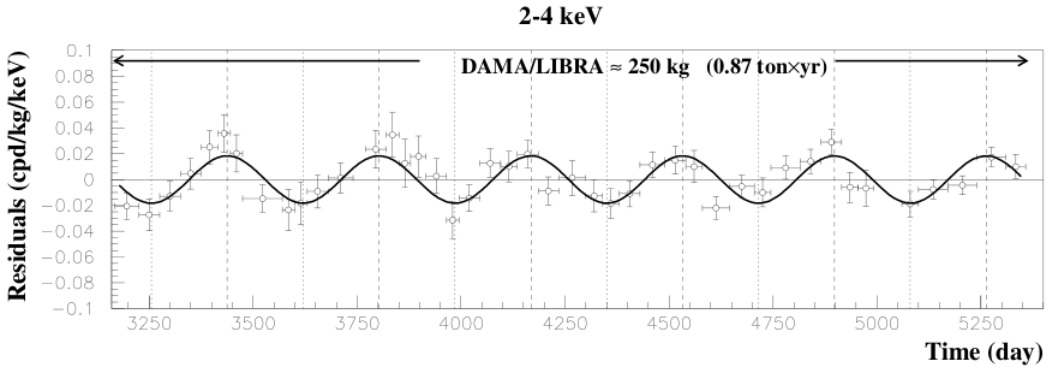

Figure 4: Experimental model-independent residual rate of the single-hit scintillation events, measured by DAMA/LIBRA in the (2 – 4) keV energy interval as a function of the time. The zero of the time scale is January 1st of the first year of data taking of the former DAMA/NaI experiment (1996). The experimental points present the errors as vertical bars and the associated time bin width as horizontal bars. The superimposed curves are the cosinusoidal functions behaviors $A\cos\omega(t-t_0)$ with period $T=\frac{2\pi}{\omega}=1$ year, with phase $t_0=152.5$ day (June 2^{nd}) and with modulation amplitudes, A, equal to the central values obtained by best fit over the whole data including also the exposure previously collected by the former DAMA/NaI experiment. Figure adapted from [9].

3 Dark Matter Theory

3.1 Lagrangian

In order to introduce dark matter and to account for the matter-dark matter interactions, one has to modify Standard Model Lagrangian by the inclusion of (among other) a $U(1)_d$ gauge group, which contains dark matter fields [10].

$$\mathcal{L} = \mathcal{L}_{SM} + \mathcal{L}_{dark} + \mathcal{L}_{kin-mix}, \tag{1}$$

Since SM particles are uncharged in this new gauge sector, all interactions with the SM are mediated by kinetic mixing of $U(1)_d$ with the photon and Z boson. The Lagrangian can then be written:

$$\mathcal{L} = \mathcal{L}_{SM} - \frac{1}{4}F^{dark}_{\mu\nu}F^{\mu\nu}_{dark} - \frac{\epsilon}{2}F^{dark}_{\mu\nu}F^{\mu\nu} + |D^{\mu}\phi|^2 - V(\phi), \tag{2}$$

where $F_{\mu\nu}$ is the photon field strength, $F^{dark}_{\mu\nu}$ is the $U(1)_d$ (dark photon) field strength, $D_\mu = \partial_\mu + ie'A'_\mu$, where A'_μ is vector gauge field, e' is $U(1)_d$ charge, $V(\phi)$ is Higgs potential. Here we omitted contribution form Z boson – $U(1)_D$ mixing.

The Lagrangian mentioned above assumes existence of dark forces field $F^{\mu\nu}_{dark}$ beyond the Standard Model and the presence of some new force-carrying boson should be expected [7]. Here comes the hypothesis of a U boson, called also a dark photon, which mass scale is in question. Once this force-carrier U is included, the possibility of new annihilation channel $\chi^+\chi^- \to UU$ opens up. This mechanism provide simple explanation for the excess of cosmic ray positrons (mentioned in section about astrophysical observations) without excess of anti-protons or photons [7]. In that reference it is also explained, that dark matter can dominantly annihilate into very hard leptons and that U cannot decay into heavier hadronic states, scalars of mass $\mathcal{O}(250MeV)$ and vectors lighter than $\mathcal{O}(1GeV)$. Also it is mentioned that cross-section of the dark matter decays into leptons can be enhanced by mechanism described by Sommerfeld.

The mass of the U boson is estimated in following way: fine-structure constant of dark matter α_{DM} is assumed to be in the order of SM fine-structure constant: $\alpha_{DM} \approx \alpha$. Weakly Interacting Massive Particles (WIMPs) of Dark Matter have mass scale selected by ATIC: 800 GeV - 1 TeV, so mass of force carrier between them should be $m_U < \alpha_{DM}M_{DM} \approx \alpha M_{DM} \sim$ GeV. That's why production of U boson particle may be reachable in flavour factories, such as DAΦNE, and can be detected by KLOE [12].

3.2 Sommerfelds enhancement

The concept of Sommerfelds enhancement originates from simple, classical reasoning: lets think abut a meteor coming towards the planet. If we "switch off" the gravity, the cross-section σ_0 for this meteor colliding with planet is equal to πR^2, where R is a radius of the planet. But if we include gravitational potential, collision cross-section

is enhanced, because meteor can be pulled towards the planed by attracting force we "switched on". For this simple example we can calculate $\sigma = \sigma_0 \left(1 + \frac{v_{esc}^2}{v^2}\right)$, where v_{esc}^2 is escaping velocity from the surface of the planet, and v is meteors velocity in infinity.

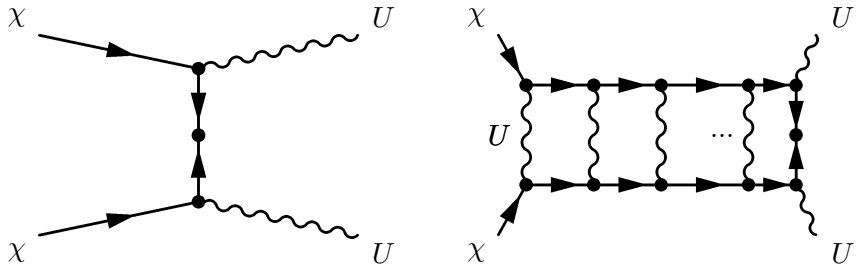

Figure 5: Diagrams of annihilation of two dark particles to two bosons $\chi\chi \to UU$, without Sommerfelds enhancement (left) and with (right). Figure adapted from [7].

Analogical phenomenon occurs, when we think in terms of quantum mechanics: cross-section for a reaction is enhanced, whenever a particle has an attractive force carrier with a Compton wavelength longer than $1/(\alpha M_{DM})$ [7]. But how this apply in our case? The cross-section for annihilation of Dark Matter particles in the centre of our galaxy should be small. However observed ATIC and PAMELA anomalies indicate large cross-section of reaction, that causes enhancement of electron/positron to appear. It is difficult to explain this phenomenon with annihilation of thermal Dark Matter, unless we include Sommerfelds enhancement, which has to occur due to velocity redshift of Dark Matter to lower values. This fact is connecting two ends of this problem: experimental observations and theory. Detailed explanation with examples upon Sommerfeld enhancement is included in appendix of reference [7]. Feynman diagram depicting this process is shown in Figure 5 (right).

3.3 More about secluded sector

A new gauge symmetry group $U(1)_d$ has been postulated and it is claimed, that it is natural to include in the theory a boson, which spontaneously breaks this symmetry, dubbed secluded Higgs-like boson h'. The dark photon mass is usually generated by Higgs mechanism, so adding this element to the theory is necessary [18]. It is not settled, which one of these two bosons is heavier, thus decay channels can be very different and detection strategies have to be different. Topology of dark Higgs decay presents Figure 6.

It is certain: in order to detect these bosons at DAΦNE facility, their masses should be less than mass of ϕ meson [11, 12].

Interesting case is when $m_{h'} < m_U, m_{h'} + m_U < m_\phi$. Then reaction: $e^+e^- \to Uh'$ and U decaying into two leptons becomes possible, so what we get is only two leptons and missing energy, because under these assumptions h' cannot decay into U. That process has a unique signature, so its detection may only be obscured by $\phi \to K_S^0 K_L^0 \to \pi^+\pi^- K_L^0$

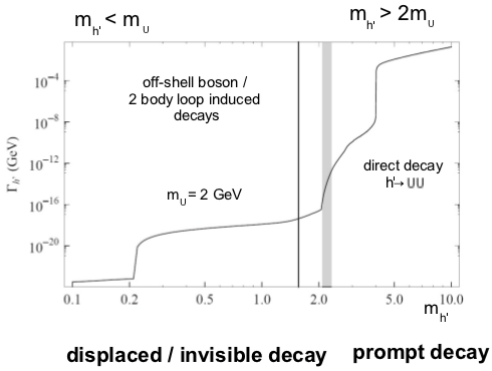

Figure 6: Higgs' decay topology depending on its mass, in GeV. Figure derived from [18].

when K_L^0 flies through the detector without interacting. If this background turns out to be a problem, one can always take data at $\sqrt{s} < 2m_K$, that can be easily done at DAΦNE, without loss of luminosity [12]. Proposed Feynman diagram of described process is shown below in Figure 7.

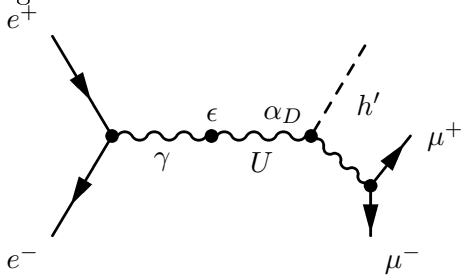

Figure 7: Feynman diagram of possible production and decay of U boson and h' through kinetic mixing with a photon (ϵ) and dark coupling α_D. Figure adapted from [18].

In the other case, when $m_{h'} > m_U$, but still $m_{h'} + m_U < m_\phi$, we get multi-lepton event, up to even 6 leptons in the final state. This is due to higgs'-strahlung process.

4 Methods of the search

There are several ways, in which we can search for manifestation U boson in non-astrophysical observations. Such earth-bound experiments can be divided into following groups:

4.1 Direct search

Direct search may be conducted in low energy and high luminosity colliders, where main reaction is: $e^+e^- \to \gamma U$, followed by $U \to \ell^+\ell^-$ (Figure 8). One can see, that U production is identical to photon, as in QED process $e^+e^- \to \gamma\gamma$, although with a much suppressed rate [19]. Reach of U boson will be available only in case of experiment, which produces large number of energetic photons. The U boson would manifest itself as a sharp peak in the invariant mass distribution of $\ell^+\ell^-$. The main background process $e^+e^- \to \gamma\ell^+\ell^-$ will result in a continuous mass distribution of the $\ell^+\ell^-$ pair. So when we observe number of events in detector, a statistically significant peak upon QED background should indicate, that dark boson appears in this reaction as well. Examples of such experiments are BaBar and Belle.

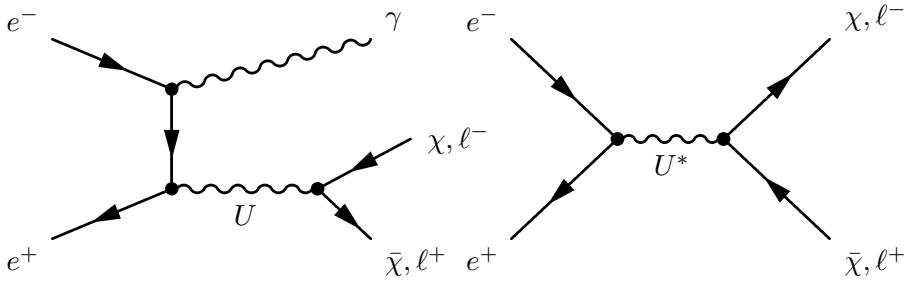

Figure 8: Production modes of light secluded-sector particles $\chi\bar{\chi}$ in e^+e^- colliders. Right: Production through an off-shell U. Left: Production of an on-shell U and a photon - the U may subsequently decay into lighter hidden-sector particles. If this sector mixes with SM sectors, U may decay into pair of leptons. For more information on kinetic mixing see the text. Figure is derived from [11].

Not only electron-positron collision gives a chance to produce the U boson. Facilities maintaining hadronic collisions also posses such opportunity. An example is a reaction initialised by two protons: $p + p \to pp + \eta,\ \eta \to U \to e^+e^-$ (WASA/CELSIUS) [13]. The $\eta \to e^+e^-$ decay has not been observed so far. An observation of the Branching Ratio significantly larger than predicted in the framework of the Standard Model would indicate an additional production mechanism including the U boson.

4.2 Decays of mesons

An existence of the U boson may manifest itself in decays of mesons, that are produced in large numbers in low energy colliders. There are many channels, through which U boson can be found. In general, a process can be denoted: $X \to Y + (U \to \ell^+\ell^-)$, with dominant background $X \to Y + \gamma^* \to Y + \ell^+\ell^-$. For X following mesons can be substituted: η, ω, ϕ, K. Such studies are conducted at experiments BESII, WASA–at–COSY, A2–at–MAMI, KLOE–at–DAϕNE. The latter experiment provides data sample of the ϕ meson, which can decay into ηU. So far the subsequent decays: $\eta \to \pi^+\pi^-\pi^0, U \to e^+e^-$ were analysed in [14]. However, to thoroughly explore all the possibilities, other decay channels of η and U are to be considered. Authors of reference [19] urge to inquiry the $U \to \mu^+\mu^-$ process, although with KLOE it is harder to reconstruct muon than electron signal.

So far decays of ϕ mesons, produced in the e^+e^- collisions were thoroughly analysed by KLOE collaboration [14]. A decay chain $\phi \to \eta U, \eta \to \pi^+\pi^-\pi^0, U \to e^+e^-$ was selected, using different cuts and background rejection. No evidence for U boson existence was found in the data sample corresponding to the luminosity of 1.5 fb^{-1}. In the mass range of $5 < M_U < 470$ MeV an upper limit of kinetic mixing parameter ϵ^2 was evaluated to be less than $2 \cdot 10^{-5}$ at 90 % confidence level. Exclusion plot with KLOE result along with other experiments is presented in Figure 9.

There are additional possible channels enabling investigation of existence of U boson, that are being currently analysed by KLOE–2 collaboration. Firstly, the other η decay channels (i.e. $\eta \to \gamma\gamma; \eta \to \pi^0\pi^0\pi^0$) will further improve calculation of upper limit of the ϵ^2 parameter, which is now known to be less than 10^{-5} at 90 % confidence level.

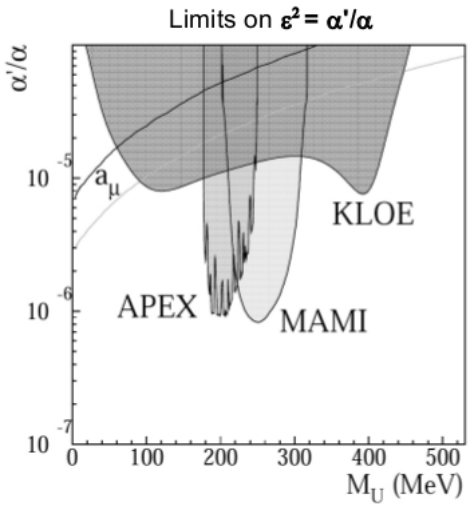

Figure 9: Exclusion plot for the parameter $\alpha'/\alpha = \epsilon^2$ with existing measurements [14, 15, 16] and limits from the muon anomalous moment a_μ [17]. Figure adapted from [18].

Secondly, there is also a higgs'-strahlung channel: $e^+e^- \to Uh'$. In the case if $m_{h'} < m_U$, then the signature of this process is a lepton-antilepton pair from the U boson decay and missing mass different from zero. The residual background contamination comes from continuum events: $e^+e^- \to \ell^+\ell^-\gamma$, and from $\phi \to K^+K^- \to \mu^+\mu^-\nu\bar{\nu}$. Last decay process can be reduced to large extent, if a run at energy below 1.02 GeV will be performed, that is no ϕ meson will be produced. The suppression of the background is expected also by improvement of KLOE-2 in the form of insertion of the inner tracker.

WASA/CELSIUS experiment in Juelich, Germany, analysed gathered data in context of decays of η meson into lepton-antilepton pairs, including assumption, that η decays also into e^+e^-. Existence of U boson would influence the branching ration for this rare process [20], but no events of $\eta \to e^+e^-$ were registered so far by this facility. This way the empirical upper limit for branching ratio was set to 5.6 $\times 10^{-6}$ at 90 % confidence level [21] and is still three order of magnitude larger than SM predictions. If indeed U boson had manifested itself as a propagator in this process, it would have increase the probability of described process. Negative result from WASA/CELSIUS decreases this way also the expected value of ϵ, showing dark matter boson being even harder to detect.

4.3 Fixed target experiments

A specific fixed target experiment is proposed by the authors of reference [19], where electron-proton interaction results in a radiation of the U boson. It is also explained, that it would increase significantly a chance of discovering the U boson because of high luminosity, achievable with this technique. Considered process proceeds as follows: $e^- + p \to e^- + U + p, U \to \mu^+\mu^-$. Another possibility arises from target experiment, which would shoot electrons in direction of a thick foil and producing U from radiation of incoming particle, then decaying to pair of leptons. Suitable facility is at Jefferson Laboratory, which conducts experiment called APEX [16].

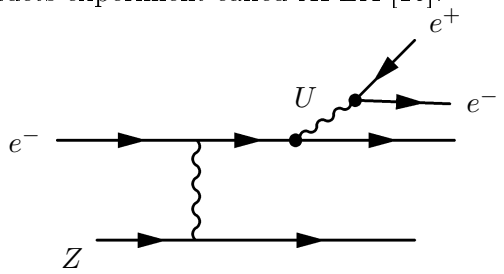

Figure 10: Production mode of light secluded-sector particle at Jefferson Laboratory from radiation of an incoming e^- beam incident on target consisting of nuclei of atomic number Z. In case of APEX experiment, an tantalum foil is used.

The A' Experiment also provided negative (so far) results of the search for U boson (or A' boson, as the authors of [16] dubbed it). The test run data allowed to search for the new particle in the range of 175-250 MeV and set the upper limit of ϵ^2 parameter to $\approx 10^{-6}$. In the contrary to method described in previous point, this measurement

assumes the simplest scenario, when electron hitting the target emits an U boson, which decays into e^+e^- pair. Detailed scheme of possible channel of production is presented in Feynman diagram in Figure 10.

4.4 Search in the continuum processes

A very interesting method can be applied in direct search of U boson, that is using events with radiated photons. This solution was so far used to measure accurately cross section of $e^+e^- \rightarrow$ hadrons [22, 23] and relies on selecting events, when electron or positron emits a photon before collision, thus lowering the energy of the e^+e^-reaction, as depicted in Figure 11.

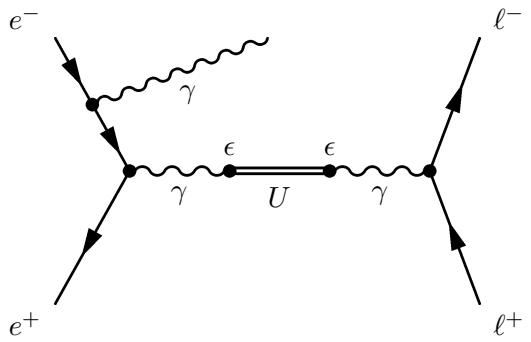

Figure 11: Examples of Feynman diagram, depicting exchange of dark photon, contributing to the process $e^+e^- \rightarrow \gamma\ell^+\ell^-$ via $e^+e^- \rightarrow \gamma\gamma^* \rightarrow \gamma U \rightarrow \gamma\ell^+\ell^-$. Scheme derived from [10].

This emission is called Initial State Radiation (ISR). In case of DAΦNE, which operates at energy $\sqrt{s} = 1.02GeV$, we deal with events occurring below that energy, so no ϕ meson is produced and there is a clear path to observe process $e^+e^-(\gamma) \rightarrow U\gamma \rightarrow \ell^+\ell^-\gamma$. In turn the FSR, stands for Final State Radiation, and, by analogy to ISR, it concerns event, in which photon was emitted from lepton or antilepton after collision, so $e^+e^- \rightarrow U(\gamma)\gamma \rightarrow \ell^+\ell^-(\gamma)\gamma$. FSR contribution to the signal can be decreased in several manners [22].

In Figure 12 an example of simulation of the invariant mass of $\mu^+\mu^-$ pair originating from the $e^+e^- \rightarrow U\gamma \rightarrow \mu^+\mu^-$ process in shown for three different assumptions of mass of the U boson and kinetic mixing parameter ϵ.

This promises, that by using this method, signatures of U boson can be found, if its mass is in the range of 0.25 - 1 GeV. For the lower mass range we can investigate process $e^+e^- \rightarrow U\gamma \rightarrow e^+e^-\gamma$.

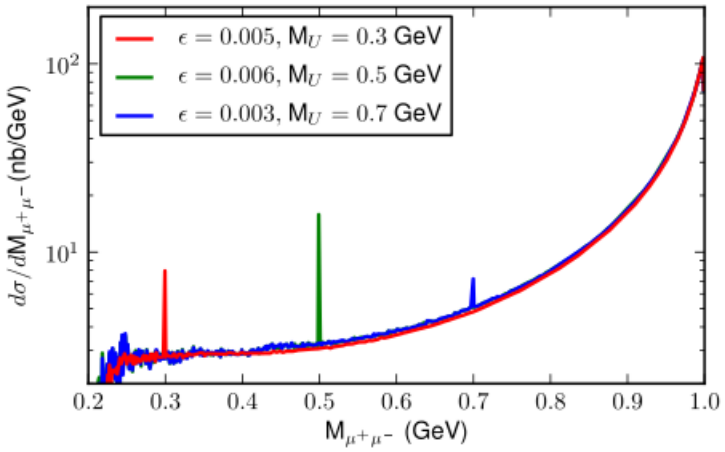

Figure 12: Simulated invariant mass distribution of the muon pairs from the $e^+e^- \rightarrow U(\gamma) \rightarrow \mu^+\mu^-(\gamma)$ for different values of the kinetic mixing parameter ϵ and U boson mass. Figure adapted from [10].

5 Cross-section evaluation

The theory of U boson existence is relatively new, so some predictions and estimations should be done, in order to gain knowledge about possibilities of detection of this particle in experiments, such as described in paragraph 4. The Quantum Field Theory provides us with method of evaluating cross-sections for various processes and this approach is applied here. Firstly, derivation of basis of this calculations in shown, then proceeded by two examples: $e^+e^- \to \mu^+\mu^-$ scattering and Bhabha events. Next in order to include U boson production, one has to move beyond standard Quantum Electrodynamics and assume additional interaction between photon and U boson. That is why the additional vertex is introduced, which symbolises kinetic-mixing described in 3.1 and defined in 8.1.

In general the differential cross-section for radiative events with photon emitted at the angle of $\phi_{min} < \phi < 180° - \phi_{min}$ is given by formulae derived from [22]:

$$\frac{d\sigma}{dM_{inv}} = \frac{4\alpha^3}{3sM_{inv}}\sigma(M_{inv})\left\{\frac{s^2+M_{inv}^4}{s(s-M_{inv}^2)}\ln\frac{1+\cos\phi_{min}}{1-\cos\phi_{min}} - \frac{s-M_{inv}^2}{s}\cos\phi_{min}\right\} \tag{3}$$

where α denotes fine structure constant, s indicates Mandelstam variable, M_{inv} is muon invariant mass and $\sigma(M_{inv})$ is total cross section for the $e^+e^- \to \mu^+\mu^-$processes.

$$|\mathcal{M}|^2 = \left| \right. \tag{4}$$

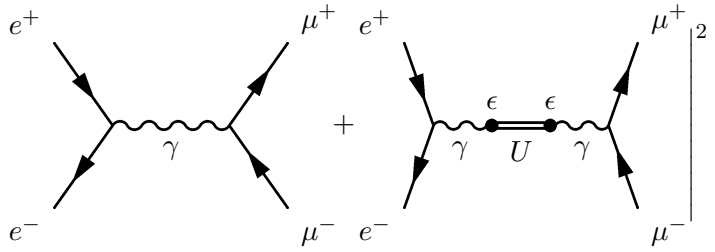

$$\left. \right|^2$$

The goal of next chapters is the derivation of the cross-section $\sigma(M_{inv})$ assuming, that the $+e^- \to \mu^+\mu^-$ process occurs via mechanisims described by the Feynman diagrams depicted above.

5.1 Introduction

Before finding a proper amplitude $\mathcal{M}$ of a process of interest, one must understand the way of calculating Feynman diagrams, which then leads to computing a process cross section σ and decay width Γ. Lets begin with writing down equations for free Dirac spinors, which can be described by ansatz [24]:

$$\psi(x) = u(\vec{p})e^{-ipx}, \tag{5}$$

where $\psi(x)$ is wave function and $u(\vec{p})$ is function of momentum vector. Inclusion of this ansatz in the Dirac equation, gives the *momentum space Dirac equation* for field operator of the particle ($u(\vec{p})$) and antiparticle ($v(\vec{p})$) respectively:

$$(\not{p} - m)u(\vec{p}) = 0, \quad \not{p} = p_\mu \gamma^\mu, \quad (\not{p} + m)v(\vec{p}) = 0, \tag{6}$$

where γ^μ are the Dirac matrices [24]. This gives two positive $u(\vec{p}, \xi)$ and two negative $v(\vec{p}, \xi)$ solutions, the latter ones are interpreted as positive-energy antiparticle solutions:

$$u(\vec{p}, \xi) = N \begin{pmatrix} \chi_\xi \\ \\ \frac{\vec{\sigma}\vec{p}}{E+m}\chi_\xi \end{pmatrix}, \quad \xi = 1, 2, \quad \chi_1 = \begin{pmatrix} 1 \\ 0 \end{pmatrix}, \quad \chi_2 = \begin{pmatrix} 0 \\ 1 \end{pmatrix} \tag{7}$$

$$v(\vec{p}, \xi) = -N \begin{pmatrix} \frac{\vec{\sigma}\vec{p}}{E+m}(i\xi^2)\chi_\xi \\ \\ (i\xi^2)\chi_\xi \end{pmatrix}, \quad \xi = 1, 2, \quad E > 0. \tag{8}$$

In the above equations $\vec{\sigma}$ is a vector made of Pauli matrices, N - normalisation constant, ξ is the index and vector number.

The complete set of equations needed to define Dirac field (spin-1/2 fermion field) reads:

$$\psi(x) = \sum_{\xi=1}^{2} \int \frac{d^3p}{\sqrt{(2\pi)^3 2E}} [u(\vec{p}, \xi)a(\vec{p}, \xi)e^{-ipx} + v(\vec{p}, \xi)a^{c\dagger}(\vec{p}, \xi)e^{ipx}] \tag{9}$$

$$\{a(\vec{p}, \xi), a^\dagger(\vec{p}, \xi')\} = \delta_{\xi\xi'}\delta(\vec{p} - \vec{p'}), \quad \{a^c(\vec{p}, \xi), a^{c\dagger}(\vec{p}, \xi')\} = \delta_{\xi\xi'}\delta(\vec{p} - \vec{p'}), \tag{10}$$

$$a^\dagger(\vec{p}, \xi')|0\rangle = |\vec{p}, \xi\rangle, \quad a(\vec{p}, \xi')|\vec{p}, \xi\rangle = |0\rangle \tag{11}$$

where $a(\vec{p}, \xi)$ and $a^{c\dagger}(\vec{p}, \xi)$ are expansion operators; $\delta_{\xi\xi'}$ is Kronecker Delta and $\delta(\vec{p} - \vec{p'})$ is Dirac Delta. Important: anticommutation relation applies for fermionic fields, for bosonic we have a commutation relation instead. All these fields are *free* and interactions are understood as their perturbations. Equation (9) is valid for fermions and for boson fields are described as follows:

Spin-0 scalar field:

$$\phi(x) = \int \frac{d^3p}{\sqrt{(2\pi)^3 2E}}[a(\vec{p})e^{-ipx} + a^\dagger(\vec{p})e^{ipx}] \tag{12}$$

Spin-1 vector field:

$$A^\mu(x) = \sum_\lambda \int \frac{d^3p}{\sqrt{(2\pi)^3 2E}}[\epsilon^\mu(\vec{p},\lambda)a(\vec{p},\lambda)e^{-ipx} + \epsilon^{\mu*}(\vec{p},\lambda)a^\dagger(\vec{p},\lambda)e^{ipx}] \tag{13}$$

where ϵ^μ is polarisation vector, which obeys $p_\mu\epsilon^\mu(\vec{p},\lambda) = 0$ and $\lambda = +, -, 0$. For massive particle moving along z-axis ($p = (E, 0, 0, |\vec{p}|)$) ϵ stands for:

$$\epsilon(\vec{p},\pm) = \mp\frac{1}{\sqrt{2}}\begin{pmatrix} 0 \\ 1 \\ \pm i \\ 0 \end{pmatrix}, \quad \epsilon(\vec{p},0) = \frac{1}{m}\begin{pmatrix} |\vec{p}| \\ 0 \\ 0 \\ E \end{pmatrix} \tag{14}$$

This way free particles of any kind are described. But we need to include interactions into picture, thus having another element of Feynman diagrams for considered processes. We are particularly interested in experimental observables such as scattering cross section and decay width. That requires transition from one state, $|\alpha\rangle$, to another, $|\beta\rangle$. This can be done by $S - matrix$, which can be perturbatively calculated (knowing the interaction Hamiltonian) with the help of Dyson series:

$$S = 1 - i\int \mathcal{H}(x_1)d^4x_1 + \frac{(-i)^2}{2!}\int \mathcal{T}\{\mathcal{H}(x_1)\mathcal{H}(x_2)\}d^4x_1d^4x_2 + ... \tag{15}$$

where $\mathcal{H}$ is particle Hamiltonian, $\mathcal{T}$ is time order operator. The matrix elements can be conveniently formulated using Feynman invariant amplitude $\mathcal{M}$:

$$\langle\beta|S|\alpha\rangle = \delta_{\beta\alpha} - i(2\pi)^4\delta^4(p_\beta - p_\alpha)\mathcal{M}_{\beta\alpha}\prod_{i=\alpha\beta}\frac{1}{\sqrt{(2\pi)^3 2E_i}} \tag{16}$$

Using introduced above Lorentz invariant amplitude $\mathcal{M}$, one may define cross-section and partial with using so called *Golden Rules* [28]:

Partial decay: $1 \to 1' + 2' + ...$ n'

$$d\Gamma = \frac{1}{2E_1}\overline{|\mathcal{M}|^2}(2\pi)^4\delta^4(p_1 - p_1' - ... - p_n')\prod_{i=1}^{n}\frac{d^3p_i'}{(2\pi)^3 2E_i'} \tag{17}$$

Differential cross section for scattering: 1 + 2 → 1' + 2' + ... n'

$$d\sigma = \frac{E_1 E_2}{\sqrt{(p_1 \cdot p_2)^2 - m_1^2 m_2^2}} \frac{1}{2E_1} \frac{1}{2E_2} \overline{|\mathcal{M}|^2} (2\pi)^4 \delta^4(p_1 + p_2 - p_1' - ... - p_n') \prod_{i=1}^{n} \frac{d^3 p_i'}{(2\pi)^3 2E_i'} \quad (18)$$

where $\overline{|\mathcal{M}|^2}$ is the amplitude averaged over unmeasured particle spins. Now equations of free particles and interactions between them have been obtained, but how do we use that knowledge for the calculations of amplitudes, based on the Feynman diagrams? In these diagrams, three elements can be distinguished: external lines (in/out channel), vertices (interactions) and propagators (internal lines). Usually a following notation is used:

1. External lines are represented by the appropriate polarisation vector or spinor:

ingoing fermion	u
outgoing fermion	$\bar{u}$
ingoing antifermion	$\bar{v}$
outgoing antifermion	v
ingoing photon	ϵ^{μ}
outgoing photon	$\epsilon^{\mu *}$
ingoing scalar	1
outgoing scalar	1

2. Vertex factor is $ie\gamma^{\mu}$, where $e\gamma^{\mu}$ is the interaction term from the Lagrangian in momentum space with all fields removed.

3. Propagator is $ig^{\mu\nu}$ where $g^{\mu\nu}$ is the inverse kinetic operator (defined by the free equation of motion) in the momentum space.

For clarity lets consider examples, which after modifications, can contribute to study actual processes $e^+e^- \to e^+e^-(\gamma), e^+e^- \to \mu^+\mu^-(\gamma), e^+e^- \to \pi^+\pi^-(\gamma)$.

5.2 $e^+e^- \to \mu^+\mu^-$ in QED

Lagrangian:

$$\mathcal{L} = \bar{\psi}(i\partial\!\!\!/ + eA\!\!\!/ - m)\psi - \frac{1}{4}F_{\mu\nu}F^{\mu\nu}, \quad F^{\mu\nu} = \partial^\mu A^\nu - \partial^\nu A^\mu \tag{19}$$

1. External lines: $e^- = u(\vec{p}_1, \xi_1), e^+ = \bar{v}(\vec{p}_2, \xi_2), \mu^- = \bar{u}(\vec{p}_3, \xi_3), \mu^+ = v(\vec{p}_4, \xi_4)$;
2. Vertices: $ie\gamma^\mu$;
3. Propagator: $\frac{-ig_{\mu\nu}}{(p_1+p_2)^2}$, $g^{\mu\nu} = \{\gamma^\mu, \gamma^\nu\}$.

These elements can be depicted in relevant diagram:

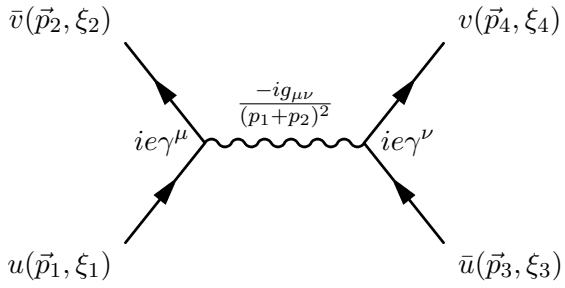

Figure 13: QED process $e^+e^- \to \mu^+\mu^-$ with $\mathcal{M}$ elements written instead of particle names. Figure adapted from [24].

$$-i\mathcal{M} = [\bar{u}(\vec{p}_3, \xi_3)(ie\gamma^\nu)v(\vec{p}_4, \xi_4)]\frac{-ig_{\mu\nu}}{(p_1+p_2)^2}[\bar{v}(\vec{p}_2, \xi_2)(ie\gamma^\mu)u(\vec{p}_1, \xi_1)] \Rightarrow \tag{20}$$

$$\Rightarrow \mathcal{M} = \frac{-e^2}{(p_1+p_2)^2}[\bar{u}_3\gamma_\mu v_4][\bar{v}_2\gamma^\mu u_1], \quad u_i \equiv u(\vec{p}_i, \xi_i),\ v_i \equiv v(\vec{p}_i, \xi_i) \quad \Rightarrow \tag{21}$$

$$\Rightarrow \overline{|\mathcal{M}|^2} = \frac{e^4}{4(p_1+p_2)^4}\sum_{\xi_{1,2,3,4}}[\bar{v}_4\gamma_\mu u_3][\bar{u}_1\gamma^\mu v_2][\bar{u}_3\gamma_\nu v_4][\bar{v}_2\gamma^\mu u_1] \tag{22}$$

In the relativistic limit $p_i \gg m_e, m_\mu$, the above formulae can be simplified applying Casimrs trick:

$$\overline{|\mathcal{M}|^2} = \frac{8e^4}{(p_1+p_2)^4}[(p_1\cdot p_3)(p_2\cdot p_4) + (p_1\cdot p_4)(p_2\cdot p_3)] \tag{23}$$

By applying the above to 18, then integrating over d^3p_4 we obtain in the centre-of-mass frame:

$$d\sigma = \frac{E_1 E_2}{\sqrt{(p_1\cdot p_2)^2 - m_1^2 m_2^2}} \frac{1}{2E_1}\frac{1}{2E_2}\frac{8e^4}{(p_1+p_2)^4}\cdot \\ \cdot[(p_1\cdot p_3)(p_2\cdot p_4) + (p_1\cdot p_4)(p_2\cdot p_3)]\cdot \\ \cdot\frac{1}{(2\pi)^2 4E_3E_4}\delta^4(E_1+E_2-E_3-E_4)\underbrace{d^3p_3}_{\vec{p}_3^2 d|\vec{p}_3| d\Omega} \quad . \tag{24}$$

After further integrating over $d^3|\vec{p}|$, we finally arrive at a desired point:

$$\frac{d\sigma_{CM}}{d\Omega} = \frac{1}{8\pi^2(E_1+E_2)^2}\frac{\vec{p}_3}{\vec{p}_1}\frac{e^4}{(p_1+p_2)^4}[(p_1\cdot p_3)(p_2\cdot p_4) + (p_1\cdot p_4)(p_2\cdot p_3)] \tag{25}$$

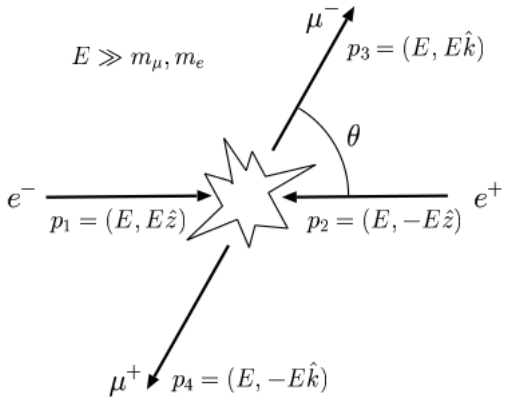

Figure 14: Scheme of collision considered in the centre-of-mass frame with defined four-momentums, energies and angles between beams and scattered particle trajectory. Figure adapted from [24].

For our particular scattering $e^+e^- \to \mu^+\mu^-$ in the centre-of-mass frame (four-momentum vectors, energies of particles and angles are defined in Figure 14). Using this notation the final formula for differential cross section:

$$\frac{d\sigma}{d\Omega} = \frac{\alpha^2}{16E^2}(1+\cos^2\theta) \tag{26}$$

where $\alpha = e^2/(4\pi)$. Further integrating over angle yields:

$$\sigma = \frac{\alpha^2}{16E^2}\int_0^{2\pi} d\phi \int_0^{\pi} \sin\theta(1+\cos^2\theta)d\theta \tag{27}$$

$$\sigma = \frac{\pi\alpha^2}{3E^2} \tag{28}$$

5.3 $e^+e^- \to e^+e^-$ Bhabha events

The Bhabha scattering rate is used as a luminosity monitor in electron-positron colliders [29], so it is important to calculate cross section for these processes. Babha scattering generates major part of events in collisions of electron and positron. There are two leading-order Feynman diagrams contributing to this interaction: an annihilation process and a scattering process. This way overall amplitude squared $|\mathcal{M}|^2$ will be derived from equation:

$|\mathcal{M}|^2 =$ (29)

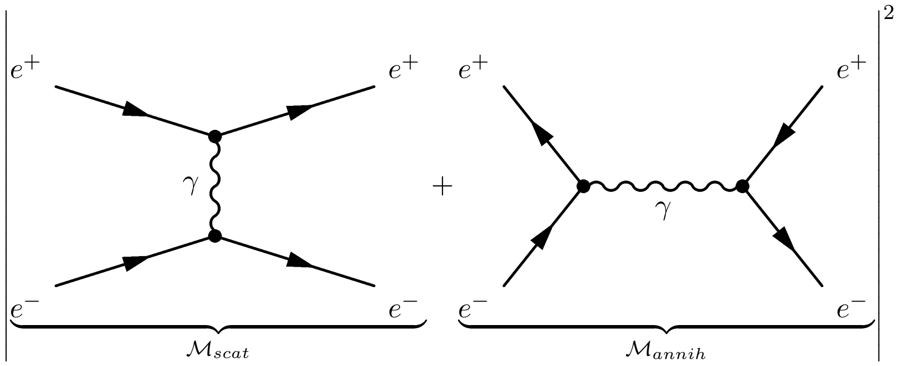

$$\frac{|\mathcal{M}|^2}{e^4} = |\mathcal{M}_{scat}|^2 - \mathcal{M}^*_{inter1}\mathcal{M}_{inter2} - \mathcal{M}_{inter1}\mathcal{M}^*_{inter2} + |\mathcal{M}_{annih}|^2 \tag{30}$$

Every component of equation (30) can be computed accordingly to the procedure described in the previous section. For more details see [29]. Much needed simplification is obtained if Mandelstams variables are introduced [24]. Then we get:

$$\frac{\overline{|\mathcal{M}|^2}}{2e^4} = \frac{u^2+s^2}{t^2} + \frac{2u^2}{st} + \frac{u^2+t^2}{s^2} \tag{31}$$

which leads inevitably to the formula for angular dependence of the cross-section expressed in terms of Lorentz invariants:

$$\frac{d\sigma}{d\cos\theta} = \frac{\pi\alpha^2}{s}\left(u^2\left(\frac{1}{s}+\frac{1}{t}\right)^2 + \left(\frac{t}{s}\right)^2 + \left(\frac{s}{t}\right)^2\right) \tag{32}$$

5.4 U boson exchange

In this section, using the rules introduced on the example of $e^+e^- \to \mu^+\mu^-$ and $e^+e^- \to e^+e^-$ processes, we will derive a formula for the cross-section of the process presented in Figure 15, which shows one of the possible processes, where a U boson may intermediate a creation of muons in the e^+e^- scattering. In this process, an energy of colliding electron and positron varies from event to event, due to the emission of the photon (Initial State Radiation), and the U boson contributes to the process in a kinetic mixing with photon.

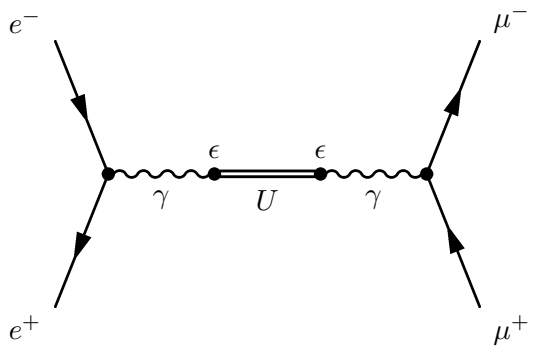

Figure 15: Feynman diagram of production of U boson through kinetic mixing with photon.

General scheme of deriving formulae for cross-section for the discussed process reads:

1. writing down Standard Model Lagrangian $\mathcal{L}_{SM}$ + kinetic mixing term
2. sketching the diagram;
3. defining incoming/outgoing particles, vertices and propagator;
4. writing down the amplitude $\mathcal{M}$ for electron-positron scattering
5. calculating $\mathcal{M}^*$;
6. calculating $\overline{|\mathcal{M}|^2}$ (sum over spins);
7. applying Casimir trick and evaluating the traces;
8. applying kinematics of centre-of-mass frame, expressing $\overline{|\mathcal{M}|^2}$ as functions of E, θ, where E is energy of electron, θ - scattering angle;
9. using golden rules for decay and scattering, thus obtaining formulae for $d\sigma$;
10. integrating over angle θ;

This way one can evaluate dependency of overall cross-section ($\sigma_U(M_{inv})$) for the process shown in Figure (15), where M_{inv} denotes invariant energy of the muon pair.
An answer for the evaluation of first step can be found in chapter 3.1, describing the Dark Matter Theory. Step 2 is the calculation of the matrix element describing the process shown in Figure 15. Definitions for amplitude elements and their derivation can be found in introduction to this part of work in chapter (5.1). All needed calculations can be found in Appendix, only step of cross-section evaluation are listed.

Step 4:

$$\mathcal{M} = [\bar{u}_3 ie\gamma^\nu v_4]\frac{-i\epsilon^2(g_{\mu\nu} - p_{6,\mu}p_{6,\nu}/m_U^2)}{p_6^2 - m_U^2}[\bar{v}_2 ie\gamma^\mu u_1] \tag{33}$$

Step 5-8:

$$\overline{|\mathcal{M}|^2} = \frac{8\epsilon^4 e^4}{(4E^2 - m_U^2)^2}[E^4(1+\cos^2\theta)+2m_e^2m_\mu^2-2E^2(m_e^2+m_\mu^2)+\frac{2E^2}{m_U^2}(4E^4+m_e^2m_\mu^2)] \tag{34}$$

Step 9:

$$\frac{d\sigma}{d\Omega_3} = \frac{\epsilon^4\alpha^2}{16(4E^2 - m_U^2)^2}\left[E^2(1+\cos^2\theta) - 2m_\mu^2 + \frac{8E^4}{m_U^2}\right] \tag{35}$$

Step 10:

$$\sigma_U = \frac{\pi\epsilon^4\alpha^2}{8(4E^2 - m_U^2)^2}\left[8E^2\frac{m_U^2 + 6E^2}{3m_U^2} - 4m_\mu^2\right] \tag{36}$$

Substituting $2E$ by M_{inv}, we obtain:

$$\sigma_U(M_{inv}) = \frac{\pi\epsilon^4\alpha^2}{4(M_{inv}^2 - m_U^2)^2}\left[M_{inv}^2\frac{m_U^2 + 1.5M_{inv}^2}{3m_U^2} - 2m_\mu^2\right] \tag{37}$$

Equation 37, implies, that for $M_{inv} \to m_U$ the cross-section rises to infinity: $\sigma_U \to \infty$. Therefore it is necessary to include in the calculations a decay width of the U boson: Γ_U. This may be accounted for by exchanging the formulae for propagator from $\frac{1}{(p_6^2-m_U^2)^2}$ to its relativistic form $\frac{1}{(p_6^2-m_U^2)^2-m_U^2\Gamma^2}$:

$$f(M_{inv}) \sim \frac{1}{(M_{inv}^2 - m^2)^2 + m^2\Gamma^2} \tag{38}$$

Finally, the total cross-section or the process, shown in the Figure 15 reads:

$$\sigma_U(M_{inv}) = \frac{0.25\pi\epsilon^4\alpha^2}{(M_{inv}^2 - m_U^2)^2 + m_U^2\Gamma_U^2}\left[M_{inv}^2\frac{m_U^2 + 1.5M_{inv}^2}{3m_U^2} - 2m_\mu^2\right] \tag{39}$$

According to [10], a decay width of the U boson to muon pair may be expressed by:

$$\Gamma_{U\to\mu^+\mu^-} = \frac{1}{3}\alpha\epsilon^2 m_U \sqrt{1-\frac{4m_\mu^2}{m_U^2}}\left(1+\frac{2m_\mu^2}{m_U^2}\right) \tag{40}$$

It is clear, that decay width depends on U boson mass m_U and kinetic-mixing parameter ϵ.

Going now back to the beginning of this paragraph, where formulae for differential cross-section is given, we find, that all components of equation 3 have been derived and now on can compute the dependence of $\frac{d\sigma}{dM_{inv}}$ for the process $e^+e^- \to \gamma\mu^+\mu^-$. For further calculations, radiation angle of the photon is assumed to be 10°, $\sqrt{s} = 1$ GeV and the variation of parameters m_U, ϵ will allow to study the phenomenon more closely. For this purpose the following graphs of differential cross-section with different values on these parameters have been plotted: 16, 17.

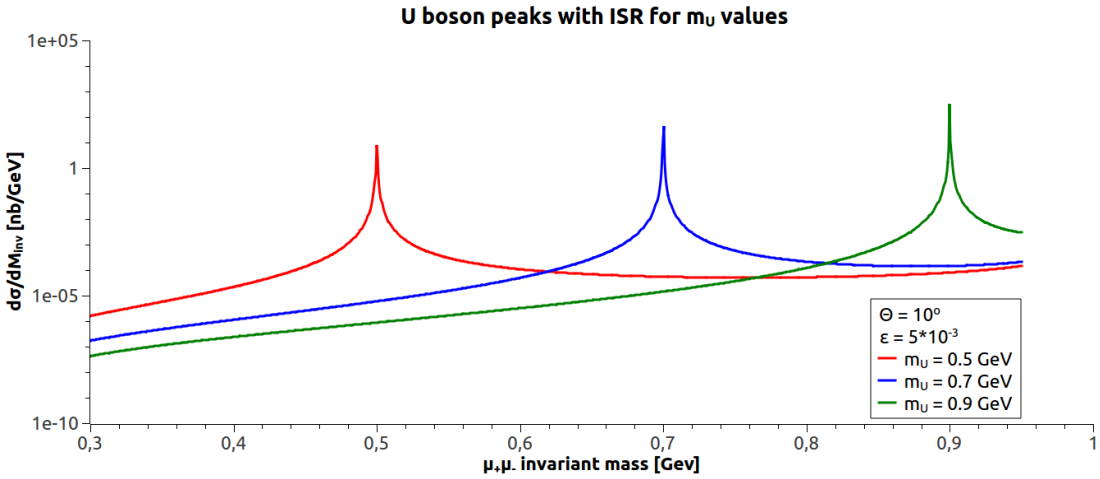

Figure 16: Graph of cross-section versus $\mu^+\mu^-$ invariant mass for different m_U values.

Graph 16 shows, that for given parameter m_U we obtain strong peak of differential cross-section. This peak of U boson resonance decreases four orders of magnitude with one order of magnitude decrease of kinetic mixing parameter ϵ, as visible in graph 17.

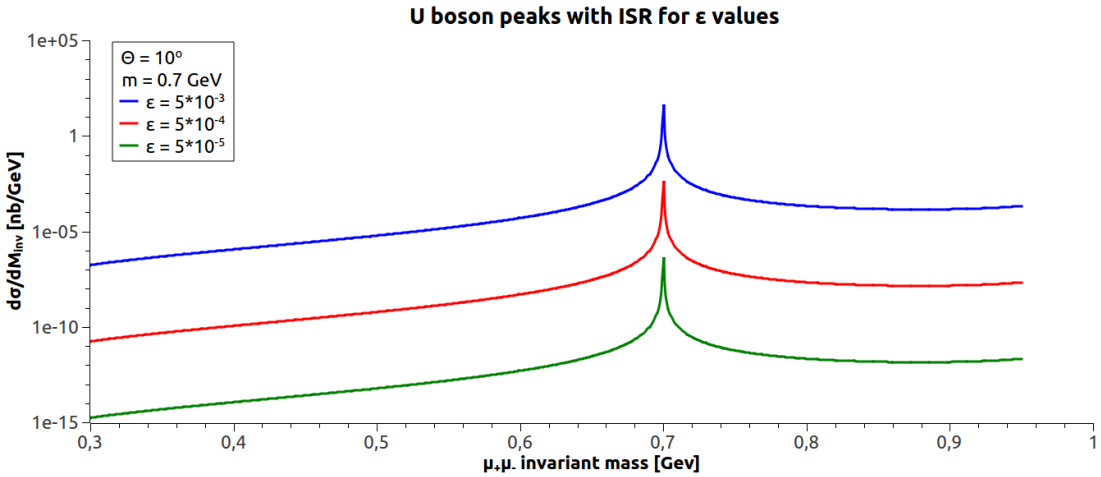

Figure 17: Graph of cross-section versus $\mu^+\mu^-$ invariant mass for different ϵ values.

5.5 Inclusion of the background

A main experimental difficulty in observing a signal from the $e^+e^- \to U(\gamma) \to \mu^+\mu^-(\gamma)$ process will be due to the unavoidable physical background, originating from the direct $e^+e^- \to \mu^+\mu^-(\gamma)$ process. However a direct production of $\mu^+\mu^-$ pairs associated with ISR will result in continuous $\mu^+\mu^-$ invariant mass distribution and a signal $e^+e^- \to U(\gamma) \to \mu^+\mu^-(\gamma)$ process may manifest itself in a form of a peak over a continuous background. The formulae 5.5 was derived from calculating the Feynman diagram:

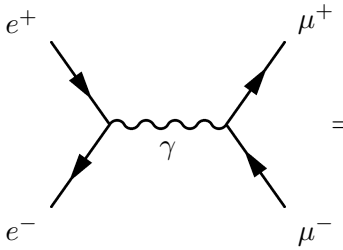

$$\Rightarrow \sigma_\mu = \frac{\pi\alpha^2}{M_{inv}^4}\left[M_{inv}^2/3 - 2m_\mu^2\right] \tag{41}$$

In Figure 18 a sum of σ_U and σ_μ is shown under the assumption, that there is no interference between these two processes [10] and that $\epsilon = 0.005$ and $m_U = 0.7$GeV.

It is clear, that cross-section for U boson production is strongly dependent on values of m_U and ϵ. These parameters influence possibility of discovering the U boson, because the higher the peak upon the $\mu^+\mu^-$ background, the easier is to recognise the signal of the boson.

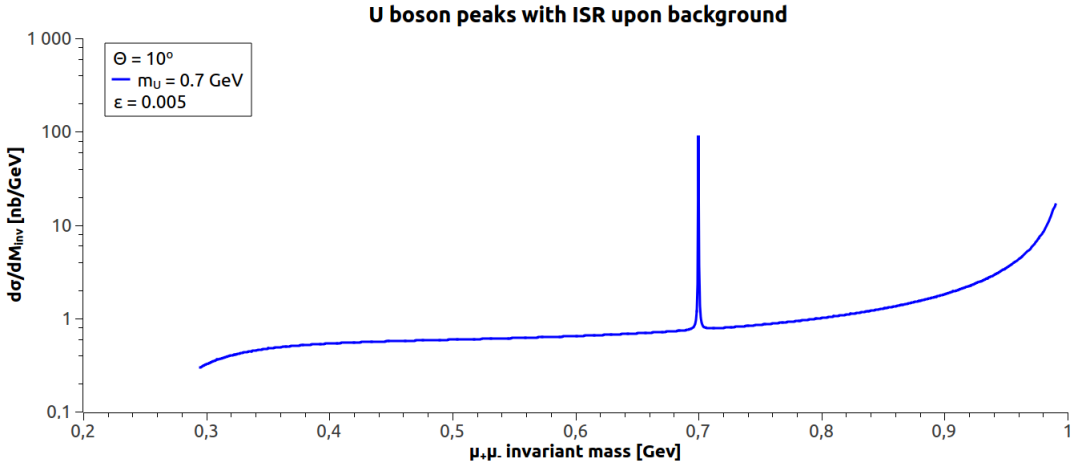

Figure 18: U boson peak upon $e^+e^- \to \mu^+\mu^-(\gamma)$ background.

5.6 Feasibility study of the U boson observation

The result of the paragraph 5.5 can be used to estimate luminosity needed to observe a signal from a U boson as a function of the mass m_U and a function of kinetic mixing parameter ϵ.

In order to state clearly, that peak of U boson signal is observed, a statistical significance at the level of at least five standard deviations would be required. The statistical uncertainty may be estimated as a square root of number of events registered in a mass range, where the signal from the U boson is expected. Defined by N_{peak} number of events corresponding to the $e^+e^- \to \gamma U \to \gamma\mu^+\mu^-$ process and by N_{QED} number of all processes (signal and background). A significance of five standard deviations will be equivalent to:

$$N_{peak} > 5\sqrt{N_{QED}}, \quad N_{peak} = \sigma_{peak} \cdot L_0, \quad N_{QED} = \sigma_{QED} \cdot L_0, \tag{42}$$

where L_0 is integrated luminosity, which can be expressed directly:

$$L_0 > \frac{25\sigma_{QED}}{\sigma^2_{peak}} \tag{43}$$

Figure 19 represents integrated luminosity in 1/pb (z axis) required to observe statistically significant signal peak (satisfying inequality 43) as a function of m_U and ϵ^2.

In Figure 20 results are presented in the exclusion plot alongside with results of other experiments. Depending on the value of m_U from 0.3 to 1 GeV, different values of ϵ^2 can be reached. It is clear, that method of searching for the U boson in the events with

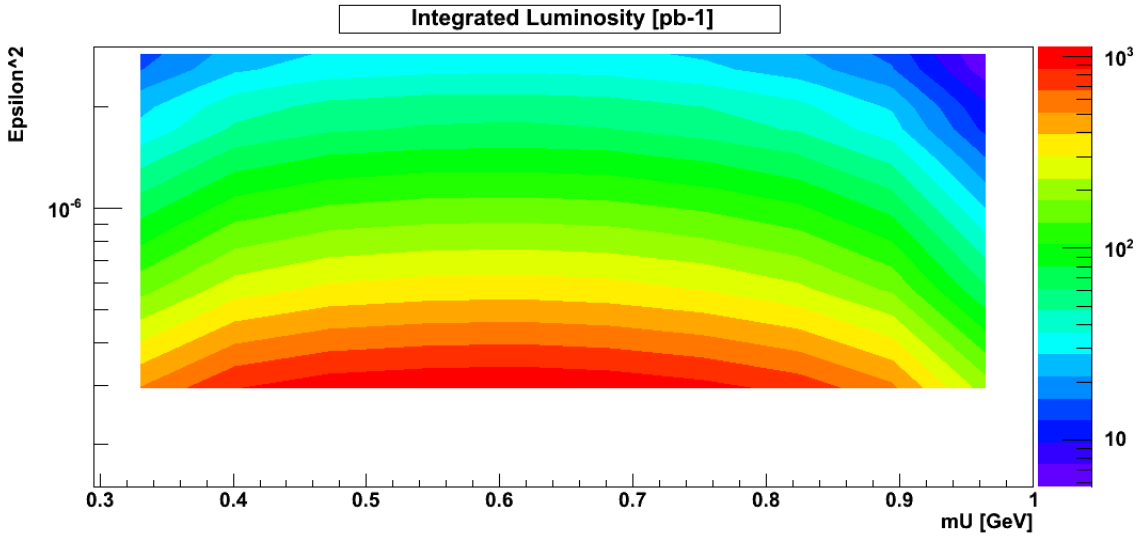

Figure 19: Representation of dependence of minimum integrated luminosity L_0 required for discovery of the U boson at 5σ level as a function U boson mass m_U and kinetic-mixing parameter ϵ. For example with L_0 equal to 1 fb^{-1}, we can discover the U boson for values of $m_U = 0.6$ GeV and ϵ up to $3 \cdot 10^{-7}$.

radiated photon, we can investigate regions of parameters, that are not tested yet, thus promising to be worthwhile.

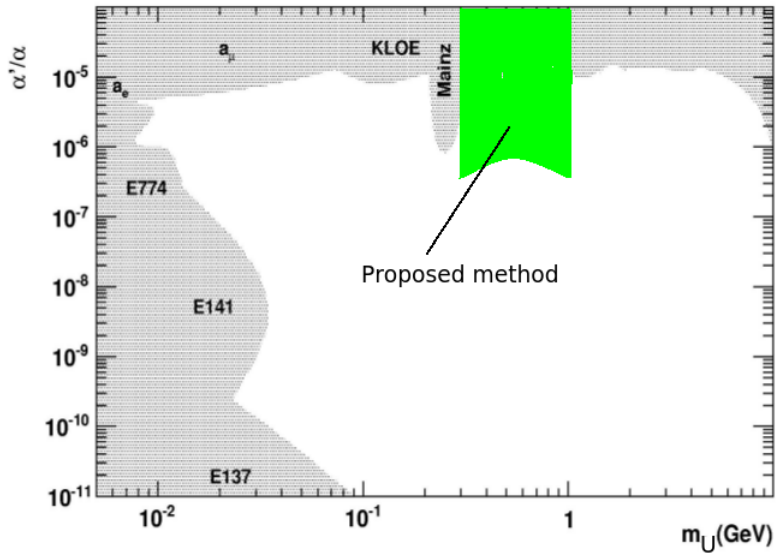

Figure 20: Exclusion plot for the parameter $\alpha'/\alpha = \epsilon^2$, compared with existing measurements and estimations derived from proposed model. Green field represents exclusion region, that can be investigated with proposed method for $L_0 = 1$ fb^{-1}.

6 Summary

Presented methods of searching for dark matter boson show, that there are many ways of conducting the investigation for finding this puzzling and elusive U particle. The theory and astrophysical observations strongly motivates existence of such boson and the experimental set-ups are being developed, in order to reach sufficient efficiency, so it seems that verification of theoretical assumptions is only a mater of time.

Main result of this thesis can contribute to the process of searching the U boson. By the use of estimation of the needed integrated luminosity, the facilities maintaining electron-positron collisions can decide how and for how long to perform the measurement.

At this point of the current research, the main goal is to cover the new regions of exclusion plot (Figure 9) with already gathered data analysis. Then proposal for specified method or experiment with adequate measurement time should be presented, taking into account theoretical model, that was evaluated here. It can be introduced in many facilities around the world, especially in Frascati, Italy, where KLOE-2 detector operates at DAΦNE collider. Analysis of data taken in the past by KLOE in context of U-to-moun decays can constitute the next step in ongoing search and the result of this analysis may serve an an indicator, what should be done in the future to improve the range of the values of the parameters. Also interesting, but more challenging possibility, is analysis of $e^+e^- \to U(\gamma) \to e^+e^-(\gamma)$ reaction, because electron-positron production constitutes large amount of events in such colliders as DAΦNE.

Possible discovery of U boson would have major consequences in the process of understanding the mysterious structure of dark matter and complex nature of particle physics. That is why it is worthy to devote time and skills in this kind of search. Author of this work admits, that beside gaining vast amount of knowledge while studying the various dark matters, the fact of tackling with problems of the universe is itself fascinating and satisfactory.

7 Acknowledgements

Author of this work would like to thank all persons, who helped the author during the writing of this thesis: Paweł Moskal, Fabio Bossi, Graziano Venanzoni, Eryk Czerwiński, Michał Silarski, Jarosław Zdebik, Izabela Balwierz, Szymon Niedźwiedzki and Mateusz Morawiec.

8 Appendix

8.1 Definitions

1. gauge boson is a particle, which obeys Bose-Einstein statistic and acts as carriers of fundamental interactions, usually as virtual particle.

2. vector boson has spin equal to 1. Scalar boson - spin 0.

3. kinetic mixing means, that there is an interaction between force mediators: photon for electromagnetic and U boson for *dark* forces. An element is added to the Lagrangian, which is a product of field tensors: $\mathcal{L}_{kin-mix} = -\epsilon F_d^{\mu\nu} F_{\mu\nu}$ [19], where ϵ is parameter deciding how strong this mixing is. In described case ϵ is considered to be small, exact value and even the order of magnitude is yet unknown.

4. hypercharge $Y = Q + I_3$, where Q is electromagnetic current and I_3 is third component of isospin. If $U(1)_d$ couples with $U(1)_Y$, we can write interaction Lagrangian with SM charged fermions: $\epsilon a_\mu J_{EM}^\mu$ [19] (where J_{EM}^μ is SM electromagnetic current); and with SM weak interacting neutral Z boson: $-\epsilon Z_\mu sin\theta_W J_d^\mu$ [19] (where J_d^μ is "dark" current).

8.2 Calculations

Detailed calculations for paragraph 5.4.

$$u_1 \equiv u(\vec{p}_1, \xi), \quad \not{\epsilon} \equiv \epsilon_\mu \gamma^\mu, \quad p_6 = p_1 + p_2 \tag{44}$$

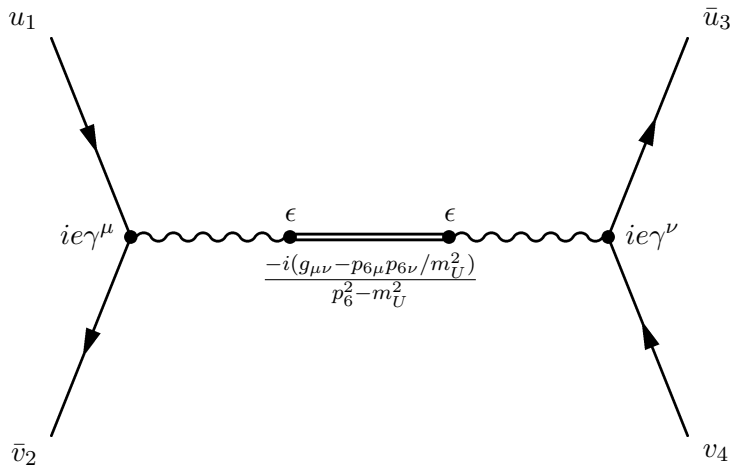

Figure 21: Feynman diagram of investigated process with $\mathcal{M}$ matrix elements indicated.

Amplitude for scattering process, with U boson production:

$$\mathcal{M} = [\bar{u}_3 ie\gamma^\nu v_4] \frac{-i\epsilon^2(g_{\mu\nu} - p_{6,\mu}p_{6,\nu}/m_U^2)}{p_6^2 - m_U^2} [\bar{v}_2 ie\gamma^\mu u_1] \tag{45}$$

$$\mathcal{M} = \underbrace{\frac{i\epsilon^2 e^2}{p_6^2 - m_U^2}}_{A} [\bar{u}_3\gamma^\nu v_4](g_{\mu\nu} - p_{6,\mu}p_{6,\nu}/m_U^2)[\bar{v}_2\gamma^\mu u_1] \tag{46}$$

$$\mathcal{M}^* = A[\bar{u}_1\gamma^\kappa v_2](g_{\kappa\lambda} - p_{6,\kappa}p_{6,\lambda}/m_U^2)[\bar{v}_4\gamma^\lambda u_3] \tag{47}$$

$$\begin{aligned} |\mathcal{M}|^2 = {} & A^2 g_{\kappa\lambda}g_{\mu\nu}[\bar{u}_1\gamma^\kappa v_2][\bar{v}_4\gamma^\lambda u_3][\bar{u}_3\gamma^\nu v_4][\bar{v}_2\gamma^\mu u_1] + \\ & -\tfrac{A^2}{m_U^2} p_{6,\mu}p_{6,\nu}[\bar{u}_1\gamma^\kappa v_2][\bar{v}_4\gamma^\lambda u_3][\bar{u}_3\gamma^\nu v_4][\bar{v}_2\gamma^\mu u_1] + \\ & -\tfrac{A^2}{m_U^2} p_{6,\kappa}p_{6,\lambda}[\bar{u}_1\gamma^\kappa v_2][\bar{v}_4\gamma^\lambda u_3][\bar{u}_3\gamma^\nu v_4][\bar{v}_2\gamma^\mu u_1] + \\ & +\tfrac{A^2}{m_U^2} p_{6,\mu}p_{6,\nu}p_{6,\kappa}p_{6,\lambda}[\bar{u}_1\gamma^\kappa v_2][\bar{v}_4\gamma^\lambda u_3][\bar{u}_3\gamma^\nu v_4][\bar{v}_2\gamma^\mu u_1] \end{aligned} \tag{48}$$

Casimir trick:

$$\sum_{spin} [\bar{u}_1\gamma^\kappa v_2][\bar{v}_2\gamma^\lambda u_1] = \mathrm{Tr}[(\not{p}_1 + m_e)\gamma^\kappa(\not{p}_2 - m_e)\gamma^\lambda] \tag{49}$$

$$\begin{gathered}\overline{|\mathcal{M}|^2} = \frac{A^2}{4} g_{\kappa\lambda} g_{\mu\nu} \mathrm{Tr}[(\not{p}_1 + m_e)\gamma^\kappa (\not{p}_2 - m_e)\gamma^\mu] \mathrm{Tr}[(\not{p}_4 - m_\mu)\gamma^\lambda (\not{p}_3 + m_\mu)\gamma^\nu] + \\ - \frac{A^2}{4m_U^2} p_{6,\mu} p_{6,\nu} \mathrm{Tr}[(\not{p}_1 + m_e)\gamma^\kappa (\not{p}_2 - m_e)\gamma^\mu] \mathrm{Tr}[(\not{p}_4 - m_\mu)\gamma^\lambda (\not{p}_3 + m_\mu)\gamma^\nu] + \\ - \frac{A^2}{4m_U^2} p_{6,\kappa} p_{6,\lambda} \mathrm{Tr}[(\not{p}_1 + m_e)\gamma^\kappa (\not{p}_2 - m_e)\gamma^\mu] \mathrm{Tr}[(\not{p}_4 - m_\mu)\gamma^\lambda (\not{p}_3 + m_\mu)\gamma^\nu] + \\ + \frac{A^2}{4m_U^4} p_{6,\mu} p_{6,\nu} p_{6,\kappa} p_{6,\lambda} \mathrm{Tr}[(\not{p}_1 + m_e)\gamma^\kappa (\not{p}_2 - m_e)\gamma^\mu] \mathrm{Tr}[(\not{p}_4 - m_\mu)\gamma^\lambda (\not{p}_3 + m_\mu)\gamma^\nu]\end{gathered} \tag{50}$$

$$\begin{gathered}\overline{|\mathcal{M}|^2} = 4A^2 [2(p_2 \cdot p_3)(p_4 \cdot p_1) + 2(p_2 \cdot p_4)(p_3 \cdot p_1) + \\ - 2m_\mu^2 (p_2 \cdot p_1) - 2m_e^2 (p_3 \cdot p) + 4m_e^2 m_\mu^2] + \\ - \frac{4A^2}{m_U^2} [2(p_2 \cdot p_6)(p_3 \cdot p_6)(p_4 \cdot p_1) - 4(p_2 \cdot p_6)(p_3 \cdot p_4)(p_1 \cdot p_6) + \\ + 2(p_2 \cdot p_6)(p_3 \cdot p_5)(p_1 \cdot p_6) - 4(p_2 \cdot p_1)(p_3 \cdot p_6)(p_4 \cdot p_6) + \\ + 2(p_2 \cdot p_1)(p_3 \cdot p_4) p_6^2 + 2(p_2 \cdot p_4)(p_3 \cdot p_6)(p_1 \cdot p_6) + \\ + 2(p_2 \cdot p_3)(p_4 \cdot p_6)(p_1 \cdot p_6) + 4m_\mu^2 (p_2 \cdot p_6)(p_1 \cdot p_6) - 2m_\mu^2 (p_2 \cdot p_1) p_6^2 + \\ + 4m_e^2 (p_3 \cdot p_6)(p_4 \cdot p_6) - 2m_e^2 (p_3 \cdot p_4) p_6^2 + m_e^2 m_\mu^2 p_6^2] + \\ + \frac{4A^2}{m_U^4} [2(p_2 \cdot p_6)(p_3 \cdot p_6)(p_4 \cdot p_6)(p_1 \cdot p_6) + \\ - (p_2 \cdot p_6)(p_3 \cdot p_4)(p_1 \cdot p_6) p_6^2 - 2(p_2 \cdot p_1)(p_3 \cdot p_6)(p_4 \cdot p_6) p_6^2 + \\ + 2m_\mu^2 (p_2 \cdot p_6)(p_1 \cdot p_6) p_6^2 - m_\mu^2 (p_2 \cdot p_1) p_6^4 + 2m_e^2 (p_3 \cdot p_6)(p_4 \cdot p_6) p_6^2 + \\ - m_e^2 (p_3 \cdot p_4) p_6^4 + m_\mu^2 m_e^2 p_6^2]\end{gathered} \tag{51}$$

Relativistic kinematics in the centre-mass frame:

$$\theta \equiv \angle(p_1, p_3), \tag{52}$$

$$p_1 = (E, \vec{p}_1); \quad p_2 = (E, \vec{p}_2); \quad p_3 = (E, \vec{p}_3); \quad p_4 = (E, \vec{p}_4); \tag{53}$$

$$\begin{gathered}p_2 \cdot p_3 = E^2(1 + \cos\theta); \quad p_2 \cdot p_4 = E^2(1 - \cos\theta); \quad p_2 \cdot p_1 = 2E^2; \\ p_2 \cdot p_6 = 2E^2; \quad p_3 \cdot p_4 = 2E^2; \quad p_3 \cdot p_1 = E^2(1 - \cos\theta); \quad p_3 \cdot p_6 = 2E^2; \\ p_4 \cdot p_1 = E^2(1 + \cos\theta); \quad p_4 \cdot p_6 = 2E^2; \quad p_1 \cdot p_6 = 2E^2; \\ p_6^2 = 4E^2.\end{gathered} \tag{54}$$

$$\overline{|\mathcal{M}|^2} = \frac{8\epsilon^4 e^4}{(4E^2 - m_U^2)^2}[E^4(1+\cos^2\theta)+2m_e^2m_\mu^2-2E^2(m_e^2+m_\mu^2)+\frac{2E^2}{m_U^2}(4E^4+m_e^2m_\mu^2)] \quad (55)$$

Golden rule for scattering cross-section:

$$d\sigma = \frac{(2\pi)^4}{(2\pi)^6 2E_1 2E_2 2E_3 2E_4 u}\overline{|\mathcal{M}|^2}dI \quad (56)$$

$$dI = \delta^4(p_1 + p_2 - p_3 - p_4)d^3p_3 d^3p_4 \quad (57)$$

$$\delta^4(p_1 + p_2 - p_3 - p_4) = \delta(p_{1,x} + p_{2,x} - p_{3,x} - p_{4,x})...\delta(E_1 + E_2 - E_3 - E_4) \quad (58)$$

$$\delta(p_{1,x} + p_{2,x} - p_{3,x} - p_{4,x})dp_{4,x} = 1, \quad etc. \quad (59)$$

$$dI = \delta(E_1 + E_2 - E_3 - E_4) \underbrace{d^3p_3}_{\vec{p}^2 d|p_3| d\Omega_3} \quad (60)$$

$$\delta(E_1 + E_2 - E_3 - E_4) = \delta(E_1 + E_2 - \sqrt{\vec{p}_3^2 + m_\mu^2} - \underbrace{\sqrt{\vec{p}_4^2 + m_\mu^2}}_{\sqrt{\vec{p}_3^2+m_\mu^2}}) \quad (61)$$

$$\delta(E_1 + E_2 - \sqrt{\vec{p}_3^2 + m_\mu^2} - \sqrt{\vec{p}_3^2 + m_\mu^2}) = \delta[f(|\vec{p}_3|)] = \frac{\delta(|\vec{p}_3| - |\vec{p}_3^0|)}{|f'(|\vec{p}_3|)|_{|\vec{p}_3|=|\vec{p}_3^0|}} \quad (62)$$

$$f'(|\vec{p}_3|) = -\frac{E_3 + E_4}{E_3 E_4}|\vec{p}_3|, \quad \delta[f(|\vec{p}_3|)] = \frac{\delta(|\vec{p}_3| - |\vec{p}_3^0|)}{|\vec{p}_3|(-E_3 - E_4)}E_3 E_4 \quad (63)$$

$$dI = \vec{p}_3^2 \frac{\delta(|\vec{p}_3| - |\vec{p}_3^0|)}{|\vec{p}_3|(-E_3 - E_4)}E_3 E_4 d|\vec{p}_3| d\Omega_3 \quad (64)$$

$$|\vec{p}_3| \to |\vec{p}_3^0| : \quad dI = \frac{|\vec{p}_3| d\Omega_3}{(E_1 + E_2)}E_3 E_4 \quad (65)$$

Cross-section in the centre-mass frame:

$$\frac{d\sigma}{d\Omega_3} = \overline{|\mathcal{M}|^2}\frac{|\vec{p}_3|}{|\vec{p}_1|}\frac{1}{64\pi^2(E_1+E_2)^2} \tag{66}$$

$$\begin{gathered}\frac{d\sigma}{d\Omega_3} = \frac{\epsilon^4\alpha^2}{16(4E^2-m_U^2)^2}\cdot \\ \cdot[E^4(1+\cos^2\theta)+2m_e^2m_\mu^2-2E^2(m_e^2+m_\mu^2)+\frac{2E^2}{m_U^2}(4E^4+m_e^2m_\mu^2)]\end{gathered} \tag{67}$$

Applying limit: $m_e \to 0$:

$$\frac{d\sigma}{d\Omega_3} = \frac{\epsilon^4\alpha^2}{16(4E^2-m_U^2)^2}\left[E^2(1+\cos^2\theta)-2m_\mu^2+\frac{8E^4}{m_U^2}\right] \tag{68}$$

Integrals:

$$d\Omega = d\phi\sin\theta d\theta, \tag{69}$$

$$\int_0^{2\pi}d\phi_3\int_0^{\pi}\sin\theta\left[E^2(1+\cos^2\theta)-2m_\mu^2+\frac{8E^4}{m_U^2}\right]d\theta = 2\pi\left[\frac{8E^2}{3}-4m_\mu^2+\frac{16E^4}{m_U^2}\right] \tag{70}$$

$$\sigma_U = \frac{\pi\epsilon^4\alpha^2}{8(4E^2-m_U^2)^2}\left[8E^2\frac{m_U^2+6E^2}{3m_U^2}-4m_\mu^2\right] \tag{71}$$

Using the dependency between energy and invariant mass of muons:

$$M_{inv}^2 = 2m_\mu^2+2(E^2-p_3\cdot p_4) = \underbrace{2m_\mu^2}_{\to 0}+4E^2 \Rightarrow M_{inv}^2 = 4E^2 \tag{72}$$

We obtain cross-section as a function of M_{inv}^2:

$$\sigma_U(M_{inv}) = \frac{\pi\epsilon^4\alpha^2}{8(M_{inv}^2-m_U^2)^2}\left[2M_{inv}^2\frac{m_U^2+1.5M_{inv}^2}{3m_U^2}-4m_\mu^2\right] \tag{73}$$

References

[1] S. van den Bergh, *The early history of dark matter* (1999) astro-ph/9904251

[2] Michał Różyczka, *Zderzenie, które wszystko wyjaśnia* (2006) Świat Nauki

[3] http://chandra.harvard.edu/photo/2006/1e0657/

[4] O. Adriani *et al.*, *Observation of an anomalous positron abundance in the cosmic radiation* (2008) Nature 458:607-609,2009 arXiv:0810.4995v1

[5] T. Philips, *Discovered: Cosmic Raysfrom a Mysterious, Nearby Object* (2008) http://science.nasa.gov/science-news/science-at-nasa/2008/19nov_cosmicrays/

[6] D. T. Cumberbatch, J. Zuntz, J.Silk, H. K. K. Eriksen, *Can the WMAP Haze really be a signature of annihilating neutralino dark matter?* (2009) arXiv:0902.0039v1

[7] N. Arkani-Hamed, D. P. Finkbiner, T. R. Slatyer, N. Weiner, *A Theory of Dark Matter* (2009) Phys.Rev.D79:015014,2009 arXiv:0810.0713v3

[8] P. Jean *et al.*, *Early SPI/INTEGRAL measurements of 511 keV line emission from the 4th quadrant of the Galaxy* (2003) arXiv:astro-ph/0309484v1

[9] R. Bernabei *et al.*, *New result from DAMA/LIBRA* (2010) Eur. Phys. J. C (2010) 67: 39-49 arXiv:1002.1028v1

[10] L. Barzé, G. Balossini, C. Bignamini, C. M. Carloni Calame, G. Montagna, O. Nicrosini, F. Piccinini, *Radiative Events as a Probe of Dark Forces at GeV-Scale e^+e^- Colliders* (2011) Eur.Phys.J.C71:1680,2011 arXiv:1007.4984v2

[11] KLOEe-2 collaboration, *Physics with KLOE-2 experiment at the upgraded DAΦNE* (2010) arXiv:1003.3868v3

[12] F. Bossi, *The role of KLOE and KLOE-2 in teh search for a secluded gauge sector* (2009) arXiv:0904.3815v1

[13] WASA/CELSIUS collaboration, *Measurement of η meson decays into lepton-antilepton pairs* (2008) Phys. Lett. D 77, 032004

[14] KLOE-2 collaboration, *Search for a vector gauge boson in ϕ meson decays with KLOE detector* (2011) arXiv:1110.0411v1

[15] H. Merkel *etal.* (A1 Collaboration) *Search for light gauge bosons of the dark sector at MAMI* (2011) Phys. Rev. Lett. 106 251802 arXiv:1101.4091

[16] APEX Experiment collaboration, *Search for a new gauge boson in the A' Experiment* (2011) JLAB-PHY-11-1406 / SLAC-PUB-14491 arXiv:1108.2750v2

[17] M. Pospelov *Secluded U(1) below the weak scale* (2009) Phys. Rev. D 80 095002 arXiv:0811.1030

[18] B. Echenard, *Hidden Sector - searches at e^+e^- colliders* (2011) presentation at Fundamental Physics Frontier, Rockville

[19] M. Reece, L-T. Wang, *Searching for the light dark gauge boson in Gev-scale experiments* (2010) JHEP 0907:051,2009 arXiv:0904.1743

[20] Paweł Moskal, *Studies of the η meson with WASA at COSYandKLOE-2 at DAFNE* (2011) arXiv:1102.5548v1

[21] Agakishiev *et al.* *η branching ratio into e^+e^-, as measured at 3.5 GeV in $p+p \to \eta + X$.* (2012) Eur. Phys. J. A48 64 (HADES Collab.)

[22] S. Binner, J.H. Kühn, K. Melnikov, *Measuring $\sigma(e^+e^- \to$ hadrons using tagged photon* (1999) Phys.Lett. B459 (1999) 279-287 arXiv:hep-ph/9902399v1

[23] G. Venanzoni, *KLOE measurement of the $\sigma(e^+e^- \to \pi^+\pi^-(\gamma))$with Initial State Radiation and the $\pi\pi$ contribution to the muon anomaly* (2009) PoS EPS-HEP2009:372

[24] K. Kumerički, *Fenman Diagrams fir Beginners* (2001) Adriatic School on Particle and Physics Informatics, Split, Croatia

[25] R. Essig, P. Schuster, N. Toro, *Probing Dark Forces and Light Hidden Sector at Low Energy e^+e^- colliders* (2009) Phys.Rev.D80:015003,2009 arXiv:0903.3941v2

[26] E. J. Chun, J-Ch. Park, *Dark matter and a new gauge boson through kinetic mixing* (2010) JHEP 1102:100,2011 arXiv:1011.3300v2

[27] KLOE-2 collaboration, *U boson searches at KLOE* (2011) arXiv:1107.2531v1

[28] F. Mandl, G. Shaw *Quantum Field Theory* (1984) ISBN 0 471 10509 0

[29] www.physics.usu.edu/Wheeler/QFT/PicsII/QFT10Mar05Bhabha.pdf

List of Figures

1 Two galactic clusters, numbered 1E0657-588. Roentgen radiation regions is coloured pink, reconstruction of dark matter distribution is blue. The gas cloud on the right is shaped like a bullet, proving, that a collision of two clusters underwent in the past. Figure adapted from chandra.harvard.edu. 3

2 PAMELA and ATIC results. Left: PAMELA positron fraction compared with theoretical model. The solid line shows a calculation by Moskalenko and Strong for pure secondary production of positrons during the propagation of cosmic-rays in the galaxy. One standard deviation error bars are shown. Figure adapted from [4]. Right: ATIC high-energy electron counts. The triangular solid curve fitted to the data comes from a model of dark-matter annihilation featuring a Kaluza-Klein particle of mass near 620 GeV; dashed line shows model without a Kaluza-Klein particle and dotted triangular curve is difference between solid and dashed line. Figure derived from [5]. 4

3 511 keV flux spectrum observed by SPI/INTEGRAL. The photon spectrum (dotted line) was obtained by fitting Gaussian function with half-width of 10°. Figure adapted from [8]. 5

4 Experimental model-independent residual rate of the single-hit scintillation events, measured by DAMA/LIBRA in the (2 – 4) keV energy interval as a function of the time. The zero of the time scale is January 1st of the first year of data taking of the former DAMA/NaI experiment (1996). The experimental points present the errors as vertical bars and the associated time bin width as horizontal bars. The superimposed curves are the cosinusoidal functions behaviors $A\cos\omega(t-t_0)$ with period $T=\frac{2\pi}{\omega}=1$ year, with phase $t_0=152.5$ day (June 2^{nd}) and with modulation amplitudes, A, equal to the central values obtained by best fit over the whole data including also the exposure previously collected by the former DAMA/NaI experiment. Figure adapted from [9]. 6

5 Diagrams of annihilation of two dark particles to two bosons $\chi\chi \to UU$, without Sommerfelds enhancement (left) and with (right). Figure adapted from [7]. 8

6 Higgs' decay topology depending on its mass, in GeV. Figure derived from [18]. 9

7 Feynman diagram of possible production and decay of U boson and h' through kinetic mixing with a photon (ϵ) and dark coupling α_D. Figure adapted from [18]. 9

8 Production modes of light secluded-sector particles $\chi\bar{\chi}$ in e^+e^- colliders. Right: Production through an off-shell U. Left: Production of an on-shell U and a photon - the U may subsequently decay into lighter hidden-sector particles. If this sector mixes with SM sectors, U may decay into pair of leptons. For more information on kinetic mixing see the text. Figure is derived from [11]. 10
9 Exclusion plot for the parameter $\alpha'/\alpha = \epsilon^2$ with existing measurements [14, 15, 16] and limits from the muon anomalous moment a_μ [17]. Figure adapted from [18]. 11
10 Production mode of light secluded-sector particle at Jefferson Laboratory from radiation of an incoming e^- beam incident on target consisting of nuclei of atomic number Z. In case of APEX experiment, an tantalum foil is used. 12
11 Examples of Feynman diagram, depicting exchange of dark photon, contributing to the process $e^+e^- \to \gamma\ell^+\ell^-$ via $e^+e^- \to \gamma\gamma^* \to \gamma U \to \gamma\ell^+\ell^-$. Scheme derived from [10]. 13
12 Simulated invariant mass distribution of the muon pairs from the $e^+e^- \to U(\gamma) \to \mu^+\mu^-(\gamma)$ for different values of the kinetic mixing parameter ϵ and U boson mass. Figure adapted from [10]. 14
13 QED process $e^+e^- \to \mu^+\mu^-$ with $\mathcal{M}$ elements written instead of particle names. Figure adapted from [24]. 19
14 Scheme of collision considered in the centre-of-mass frame with defined four-momentums, energies and angles between beams and scattered particle trajectory. Figure adapted from [24]. 20
15 Feynman diagram of production of U boson through kinetic mixing with photon. 22
16 Graph of cross-section versus $\mu^+\mu^-$ invariant mass for different m_U values. 24
17 Graph of cross-section versus $\mu^+\mu^-$ invariant mass for different ϵ values. . 25
18 U boson peak upon $e^+e^- \to \mu^+\mu^-(\gamma)$ background. 26
19 Representation of dependence of minimum integrated luminosity L_0 required for discovery of the U boson at 5σ level as a function U boson mass m_U and kinetic-mixing parameter ϵ. For example with L_0 equal to 1 fb^{-1}, we can discover the U boson for values of $m_U = 0.6$ GeV and ϵ up to $3 \cdot 10^{-7}$. 27
20 Exclusion plot for the parameter $\alpha'/\alpha = \epsilon^2$, compared with existing measurements and estimations derived from proposed model. Green field represents exclusion region, that can be investigated with proposed method for $L_0 = 1$ fb^{-1}. 27
21 Feynman diagram of investigated process with $\mathcal{M}$ matrix elements indicated. 30